Journal of Membrane Science & Research

journal homepage: www.msrjournal.com

Research Paper

Hydroxyl-functionalized Covalent Organic Framework Membranes: Fast Organic Solvent Nanofiltration

Digambar B. Shinde [1†], Li Cao [1†], Sushil Kumar [1], Zongyao Zhou [1], I-Chun Chen [1], Dinga Wonanke [2], Matthew Addicoat [2], Zhiping Lai [1,*]

[1] *Division of Physical Science and Engineering, King Abdullah University of Science and Technology (KAUST), Thuwal, 23955-6900, Saudi Arabia*
[2] *School of Science and Technology, Nottingham Trent University, Nottingham, NG11 8NS, UK*
[†] *These authors contributed equally to this study*

Article info

Received 2021-12-28
Revised 2022-03-14
Accepted 2022-03-19
Available online 2022-03-19

Keywords

COF
Membranes
Surface chemistry
Organic solvent nanofiltration
Mass transport mechanism

Highlights

- Ultrathin COF membranes with different chemical properties are prepared.
- The introduction of polar hydroxyl groups enhances the solvent permeability.
- The transport mechanism through COF membranes is investigated.

Graphical abstract

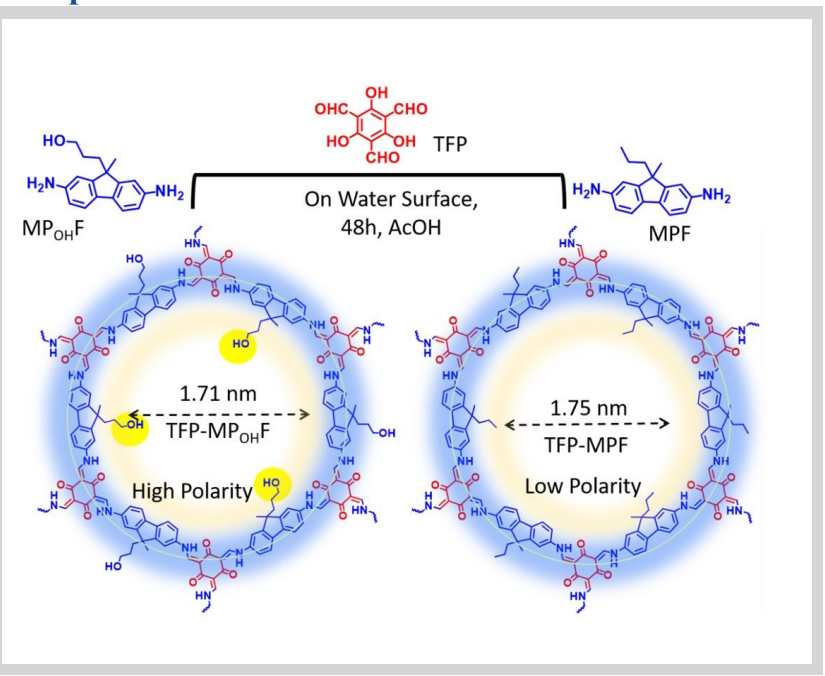

Abstract

Two-dimensional covalent organic framework (COFs) membranes have shown promise for organic solvent nanofiltration applications. However, the ability to modulate the chemical properties of the membranes and their effects on the molecular transport process has not yet been explored. Here, we demonstrate the synthesis of two COF membranes (TFP-MP$_{OH}$F and TFP-MPF) with the same scaffold structures but different internal chemical properties. The presence of hydroxyl groups in the TFP-MP$_{OH}$F membranes resulted in a significant improvement in polar solvent permeability. In contrast, the hydrophobic TFP-MPF membranes offered excellent permeability to nonpolar solvents, which was 130 – 235% higher than the TFP-MP$_{OH}$F and commercial polymeric membranes. In addition, both COF membranes exhibited precise molecular sieving capacity with an apparent molecular weight cut-off (MWCO) of 800 g mol^{-1} and excellent stability. A deviation from the pore-flow model was observed for the TFP-MP$_{OH}$F membranes, which was due to the specific interactions between solvent molecules and polar channel walls.

1. Introduction

Organic solvent nanofiltration (OSN) has gained much appeal in recovering organic solvents from waste in the chemical, textile, and pharmaceutical industries due to its superior energy efficiency, attractive economic feasibility, and environmental friendliness [1-6]. However, the solvent permeability and molecular sieving capacity of current OSN membranes are very limited due to the nature of the amorphous polymer

* Corresponding author: Zhiping.lai@kaust.edu.sa (Zh. Lai)

DOI: 10.22079/JMSR.2022.545623.1524

membranes used, which are generally dense and unstable in organic solvents [6-9]. In this context, crystalline materials with well-defined pore structures have great potential to overcome the permeability-selectivity trade-off which exists in polymeric membranes [10-14]. Covalent organic frameworks (COFs) have been recognized as alternative membrane materials due to their well-defined pore structures and tunable pore size, which can simultaneously achieve high flux and high selectivity [15-20]. Currently, researchers are mainly focusing on the fabrication of ultrathin, defect-free COF membranes with high crystallinity [21-26]. These ultrathin crystalline COF membranes have been shown to have very high solvent flux as well as considerable molecular sieving capacity [27,28]. Considerable efforts have also been made to correlate solvent permeability with the pore size of COF membranes [25]. Banerjee et al. fabricated crystalline COF membranes showing pore diameters between 3.0 and 1.6 nm by designing monomers with different lengths and observed corresponding changes in solvent permeance were observed [29, 30]. In our previous work, we developed crystalline COF membranes possessing pore diameters between 1.7 and 0.9 nm by using different lengths of carbon chains. This has improved our fundamental understanding of the relationship between pore size and molecular separation efficiency [15,31,32].

However, the specific interactions between solvent molecules and channel walls also play an important role in molecular separation [9,33,34]. A fundamental understanding of solvent-COF interactions and the mechanism of the mass transport through COF membranes is particularly important for the development of high-performance membranes for OSN applications. Although recent simulation studies have shown the significant effects of surface chemical properties of COF membranes on solvent permeability and solute rejection [35,36], experimental demonstrations are still rare. Here, two innovative diamine monomers, 9-methyl-9-propyl-9H-fluorene-2,7-diamine (MPF) and 3-(2,7-diamino-9-methyl-9H-fluoren-9-yl) propan-1-ol ($MP_{OH}F$) were synthesized and had an identical molecular structure but different pendant groups. Subsequently, the two COF membranes, TFP-$MP_{OH}F$ and TFP-MPF were prepared, with the same framework structure but different internal chemical properties. The TFP-$MP_{OH}F$ membranes have relatively hydrophilic channels with flexible polar hydroxyl groups on their pore walls, which have a favorable affinity for polar solvents. On the other hand, the alkyl groups make the TFP-MPF membranes relatively hydrophobic so that they exhibit higher permeability to nonpolar solvents. The mechanism of solvent transport also correlated with the chemical properties of both COF membranes.

2. Experimental Section

2.1 Preparation of COF Membranes

The procedure for synthesizing monomers (MPF and $MP_{OH}F$) is provided in the supporting information (Precursor synthesis). TFP-MPF and TFP-$MP_{OH}F$ membranes were prepared by a Schiff base condensation reaction on the air-water interface. First, the stock solutions of precursors were prepared. TFP (6.3 mg) was dissolved in toluene (10 mL), and MPF (11.37 mg) was dissolved in toluene (10 mL), whereas the other diamine precursor $MP_{OH}F$ (12.06 mg) was dissolved in a mixture of toluene (8 mL) and acetonitrile (2 mL) in the presence of a catalytic amount of acetic acid (0.5 mL) at room temperature. The TFP and MPF/$MP_{OH}F$ solutions were mixed well and then sonicated at room temperature for 15 minutes (Fig. S1). For the synthesis of two COF membranes, the resulting amount of solution (0.05 to 0.20 mL) was carefully dropped onto the water surface using a micropipette. The reaction bottles were capped and kept for 48 hours at 20 ºC. The unceasing light yellow film of both COFs was formed on the water surface after the completion of the reaction. By changing the volume of the precursor solutions, the membrane thickness could be controlled from 20 to 80 nm (Fig. S1b). The formed COF membrane was carefully transferred to a silicon wafer, polymer support, or anodic aluminum oxide (AAO) disk and dried at room temperature. The detailed characterization of the membranes is provided in the supporting information (Membrane characterization).

2.2 Permeance studies

OSN measurements were performed using a homemade dead-end filtration system. A series of polar and nonpolar solvents were added to the feed chamber and then passed through the membrane at 25 °C, applying a transmembrane pressure of 1 bar. After waiting for 2 h until a stable flux was reached, the solvent permeate was collected, and the solvent permeance was calculated as follows,

$$P = V / (A.\Delta t.\Delta p) \quad (1)$$

where V is the solvent volume; A, Δt, Δp, Prefer to the effective area, permeation time, applied pressure, and solvent permeance, respectively.

The molecular weight cut-off (MWCO) of COFs membranes was investigated by separating a series of dyes. A stock solution of each dye was prepared at a concentration of 50 ppm. The dye solution was added to the feed chamber of the same filtration setup in which the OSN measurements were performed. The volume of the feed side is about 2 L, which is sufficient to keep the feed concentration almost constant during the study period. Dye rejection was calculated,

$$R = (1 - C_P / C_F) \times 100\% \quad (2)$$

where C_P and C_F refer to the permeate and feed concentration, respectively.

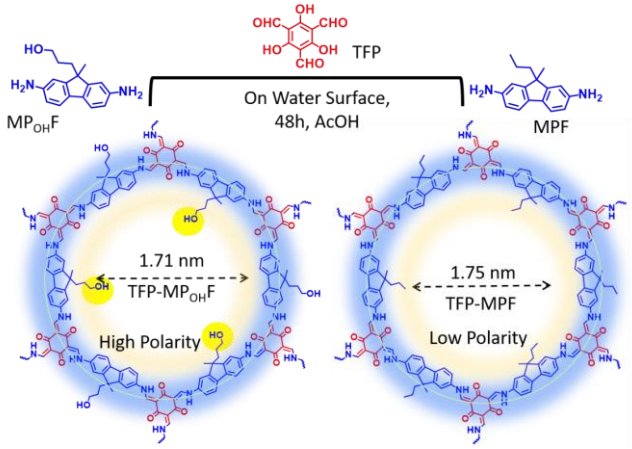

Fig. 1. The synthesis of TFP-$MP_{OH}F$ and TFP-MPF by a Schiff-base condensation reaction.

3. Results and discussion

The TFP-$MP_{OH}F$ and TFP-MPF membranes were fabricated by condensation of 9-methyl-9-propyl-9H-fluorene-2,7-diamine (MPF) or 3-(2,7-diamino-9-methyl-9H-fluoren-9-yl) propan-1-ol ($MP_{OH}F$) and 1,3,5-triformylphloroglucinol (TFP) on water surface, respectively. Typically, a certain volume of the precursor solution containing monomers and acetic acid was dropped on the water surface. The polymerization reaction was engaged at room temperature for 48 h to allow the two monomers (Figs. 1 and S1a). The thickness of the membranes can be well regulated from 20 to 80 nm by adjusting the volume of the precursors (Fig. S1b). The resulting COF membranes were robust enough to be transferred onto various substrates for structural characterization and solvent permeation experiments. Both surface and cross-sectional SEM images showed that the synthesized TFP-$MP_{OH}F$ and TFP-MPF membranes were compact and defect-free (Fig. 2).

The crystallinity of TFP-$MP_{OH}F$ and TFP-MPF membranes was investigated by X-ray powder diffraction (PXRD). The PXRD patterns of TFP-$MP_{OH}F$ and TFP-MPF showed reflection peaks at 5.8, 10.1, 15.4, and 23-28° corresponding to the (100), (100), (220), and (001) reflection planes, respectively (Figs. 3a and d). The presence of broad peaks around 23-28° was attributed to the bulky alkyl groups within the pores [32]. All possible simulated structures were prepared using the self-consistent charge density-functional tight-binding method (SCC-DFTB) with London dispersion corrections, and the correct unit cells were determined (Fig. 3b, c for TFP-$MP_{OH}F$ and Fig. 3e, f for TFP-MPF) [32,37]. The diffraction pattern of the prepared COF membranes resembled that of an inclined eclipsed-stacking model. Pawley refinement was performed to determine the exact unit cell parameters. It was found that there was little difference between the experimental and simulated PXRD patterns. The unit cell values are refined: (a = 26.54 Å, b = 26.34 Å, c = 15.03 Å; α = 40.05°, β = 89.52°, γ = 119.52°; Rwp = 5.02 %, Rp = 8.61 %) for TFP-$MP_{OH}F$, (a = 26.19 Å, b = 25.93 Å, c = 14.93 Å; α = 38.99°, β = 90.37°, γ = 119.26°; Rwp = 5.11 %, Rp = 9.21 %) for TFP-MPF.

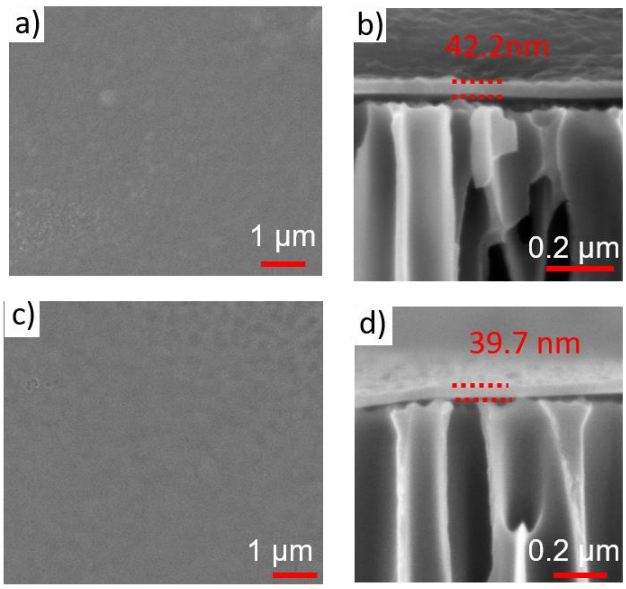

Fig. 2. Surface (a) and cross-section (b) SEM images of TFP-MP$_{OH}$F; Surface (c) and cross-section (d) SEM images of TFP-MPF.

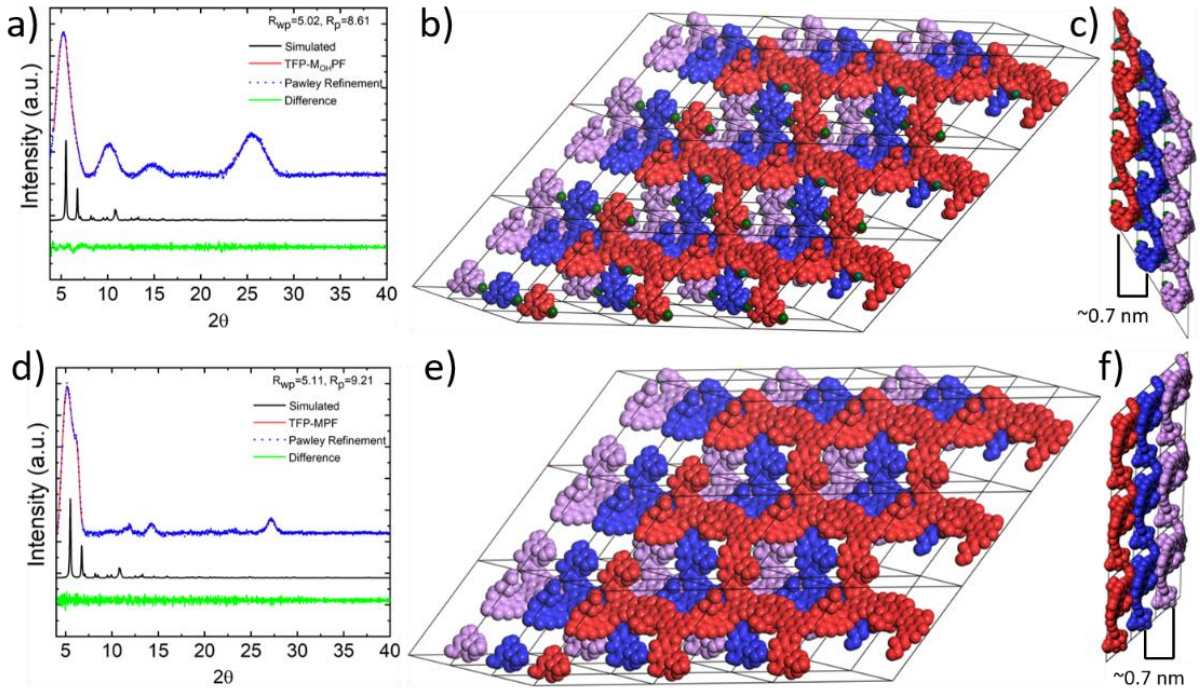

Fig. 3. (a) The both (simulated and experimental) PXRDs of TFP-MP$_{OH}$F and their fitting pattern results; (b and c) top face and side view of TFP-MP$_{OH}$F simulated structure, respectively; (d) the both (simulated and experimental) PXRD patterns of TFP-MPF; (e, f) top face and side view of TFP-MPF simulated structure, respectively.

The formation of *β*-ketoenamine bonds in both COF membranes was confirmed using Fourier transform infrared spectroscopy (FT-IR) by the presence of the characteristic stretching peaks of the –C=O and −C−N bonds at 1577-1589 and 1254 cm-1, respectively (Fig. 4a, b) [15]. The chemical structure of the as-prepared COF membranes was also confirmed by XPS (X-ray photoelectron spectroscopy). The C 1s (high-resolution profile) at 284.37, 284.76, 286.41, and 287.79 eV were attributed to C=C, C-C, C-O, and C=O, respectively. The peak at 399.99 eV (N 1s) was assigned to C-NH bonds, and the O 1s peaks at 531.24 and 532.62 eV were attributed to C=O and C-O bonds, respectively. The XPS results further confirmed the formation of *β*-ketoenamine bonds (Fig. S2). Moreover, the ^{13}C CP-MAS NMR solid-state spectrum of TFP-MP$_{OH}$F and TFP-MPF showed the characteristic signals at 183.8 and 184.2 ppm, corresponding to the *β*-ketoenamine linkage (Fig. 4c, d) [38].

The pore size distribution of two COF membranes was determined using the non-local density function theory (NLDFT). The measured pore size was 1.67 and 1.71 nm for the TFP-MP$_{OH}$F and TFP-MPF membranes, respectively (Fig. 4e, f), which was in good agreement with the simulated values (Fig. S3). The Brunauer-Emmett-Teller (BET) surface areas were 324 m^2 g^{-1} (Fig. 4g) and 345 m^2 g^{-1} (Fig. 4h) for TFP-MP$_{OH}$F and TFP-MPF membranes, respectively. The water contact angles of TFP-MP$_{OH}$F and TFP-MPF membranes are 61.0° and 78.3°, respectively (Fig. S4), indicating that the TFP-MP$_{OH}$F membrane is more hydrophilic owing to the presence of hydroxyl groups.

COF membranes were then deposited onto the anodic aluminum oxide (AAO) support (pore size: 20 nm) for organic solvent permeation measurements. Considering that TFP-$MP_{OH}F$ and TFP-MPF membranes have different chemical structures, both polar and nonpolar solvents were tested for their permeance through COF membranes. The TFP-$MP_{OH}F$ membrane showed high permeance to polar solvents: acetonitrile (442 LMH bar^{-1}), methanol (376 LMH bar^{-1}), water (343 LMH bar^{-1}), ethanol (165 LMH bar^{-1}), and moderate permeance to nonpolar solvents: heptane (124 LMH bar^{-1}) and hexane (97 LMH bar^{-1}), as shown in Fig. 5a. The TFP-MPF membrane showed a similar transport trend but slightly lower permeance for polar solvents in the order acetonitrile (302 LMH bar^{-1}) > methanol (218 LMH bar^{-1}) > water (128 LMH bar^{-1}) > ethanol (101 LMH bar^{-1}). The higher permeance performance of the TFP-$MP_{OH}F$ membrane can be attributed to the relatively hydrophilic channels with hydroxyl groups, which have a favorable affinity for polar solvents. In contrast, the TFP-MPF membranes have relatively hydrophobic channels, resulting in higher permeance to nonpolar solvents such as hexane (384 LMH bar^{-1}) and heptane (286 LMH bar^{-1}), which are four and two times higher than the TFP-$MP_{OH}F$ membranes, respectively. Note that both the TFP-$MP_{OH}F$ and TFP-MPF membranes have exceptionally high permeation performance for organic solvents compared to previously reported membranes (Table S1). In particular, the TFP-$MP_{OH}F$ membrane has methanol permeance of 376 LMH bar^{-1}, ~ 780-folds higher than the commercial DuraMem DM150 membrane (0.48 LMH bar^{-1}) [6]. The ultra-high solvent flux is ascribed to the intrinsic microporosity and ordered structure of the COF materials, which promote rapid solvent transport.

Subsequently, the molecular transport mechanism through COF membranes was investigated. The permeance of various solvents of the TFP-MPF membrane was first plotted along with their viscosity in Fig. 5b. Remarkably, the solvent permeance is linearly proportional to the reciprocal of viscosity ($1/\eta$), indicating negligible interactions between the solvents and the channel walls in TFP-MPF membranes [8]. The solvent permeance is estimated by the Hagen-Poiseuille equation, $P=n\pi d^4/128\eta L\tau$. Moreover, the production of permeance and viscosity is independent of the total Hansen solubility parameters, as shown in Fig. 5c, indicating that the behavior of solvent transport through TFP-MPF membranes follows the pore-flow model. This finding is consistent with our previously reported COF membranes with alkyl chains [15, 31]. However, the TFP-$MP_{OH}F$ membranes show a distinct trend, i.e., the production of permeance and viscosity increases linearly with the total Hansen solubility parameters (Fig. 5d). This linear correlation deviates from the pore-flow behavior and the Hagen–Poiseuille law will not be applicable to TFP-$MP_{OH}F$ membranes. Such a deviation has been observed for ceramic and dense polymeric membranes, indicating that there exist interactions between the channel walls and the solvents [34]. It should be noted that the favorable affinity for solvents, especially polar solvents, has promoted the permeation performance of TFP-$MP_{OH}F$ membranes with ordered channel structures. While the strong interactions between dense polymeric membranes and solvents usually result in high transport resistance [6].

The molecular sieving capacity of TFP-$MP_{OH}F$ and TFP-MPF membranes was investigated using a variety of dye molecules with a wide range of molecular dimensions. These dyes were dissolved in water and methanol as feed solutions, respectively. The 3D bulky chemical structures of the dyes with their molecular weights (139-1314 DA) and molecular dimensions are shown in Fig. S5. Since the membranes of TFP-$MP_{OH}F$ and TFP-MPF have comparable pore sizes, they showed similar rejection behavior with a sharp cut-off value molecule weight of around 800 g mol^{-1} (Fig. 6a). The separability of the membrane is usually defined by the MWCO and the rejection rate is 90%. In contrast, the inclination of the sieve is determined via the MWRO and the rejection rate is 10%. It can be seen that MWCO and MWRO are 800 and 650 Da, respectively (Fig.6a). The small variation between MWCO and MWRO of the two membranes is because the COF membrane has a very short molecular sieve because of its well-ordered crystalline structure. The zeta potential results indicated that both TFP-$MP_{OH}F$ (-11 mV) and TFP-MPF (-8 mV) membranes are negatively charged at neutral conditions (Fig. S6). Since the ionic dyes can not be dissociated in common organic solvents, and the electrostatic repulsion mechanism can be excluded. Therefore, dye separation is determined by size exclusion. The selective removal of dye molecules (NP) from dye mixtures (NP and RG) was also demonstrated. For this purpose, a TFP-$MP_{OH}F$ membrane was sandwiched between two glass chambers. One chamber was filled with RG and NP (1:1, v/v), while the other was filled with fresh methanol. Since RG is blue and NP is yellow, mixing these two dyes results in a green mixture (Fig. S7a). After 24 hours, the left chamber turns yellow, indicating that only NP can pass through the TFP-$MP_{OH}F$ membrane, while the larger RG molecules were blocked (Fig. S7b).

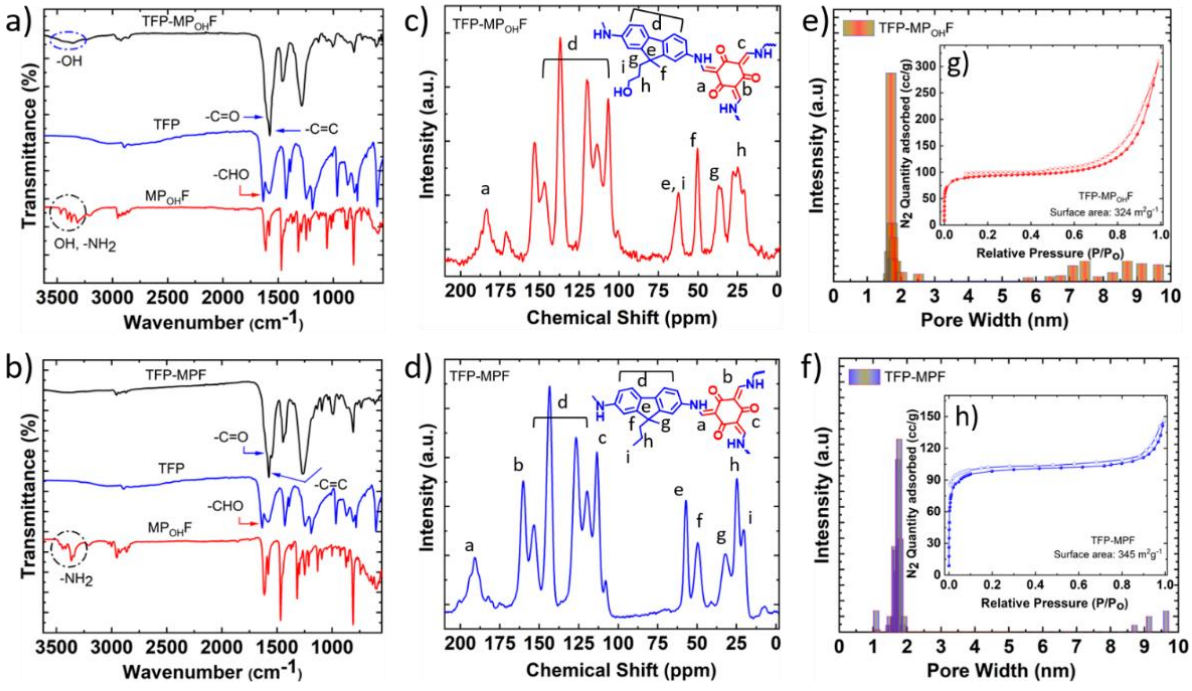

Fig. 4. FT-IR spectra of COF TFP-$MP_{OH}F$ (a) and COF TFP-MPF (b) the corresponding monomers (TFP, $MP_{OH}F$, and MPF), respectively; ^{13}C CP-MAS spectra of COF TFP-$MP_{OH}F$ (c) and COF TFP-MPF (d), respectively; pore size distribution of COF TFP-$MP_{OH}F$ (e) and COF TFP-MPF (f), respectively; N_2 sorption isotherm of TFP-$MP_{OH}F$ (g) and TFP-MPF (h), respectively.

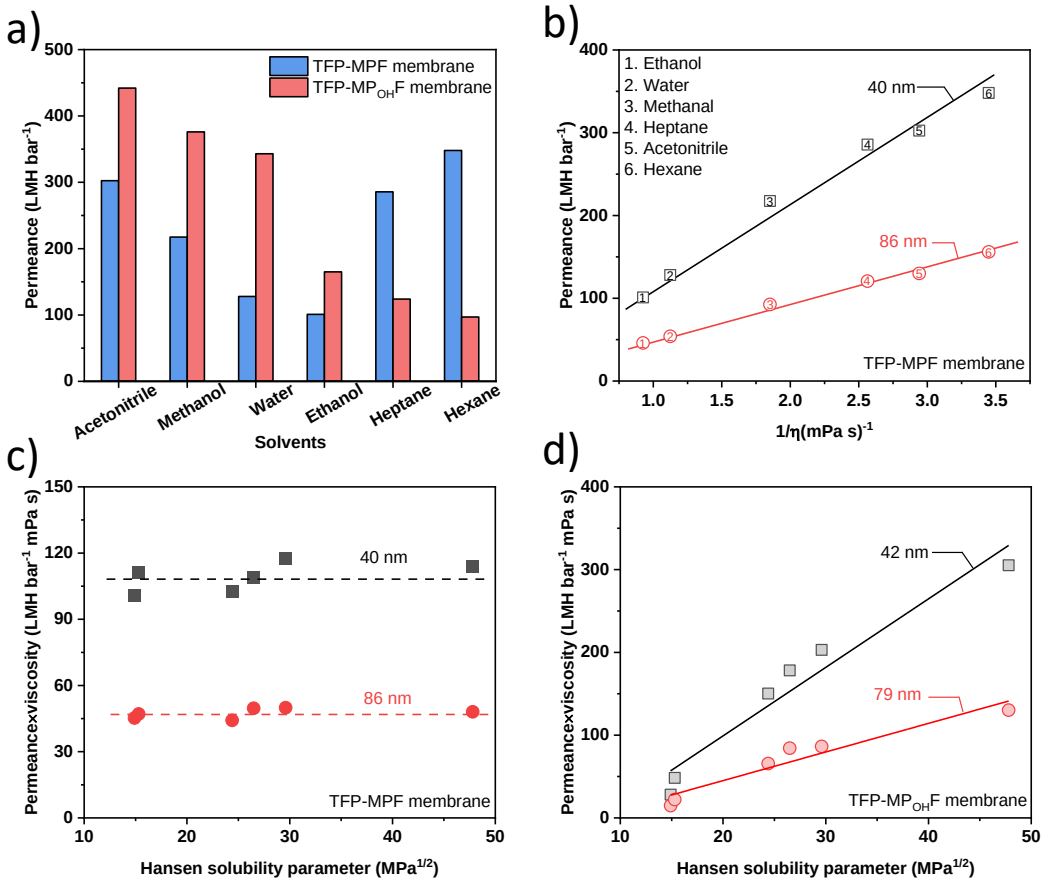

Fig. 5. (a) The polar and nonpolar solvent permeances of TFP-MP$_{OH}$F and TFP-MPF membranes. (b) Permeance as a function of the inverse of solvent viscosity. Production of solvent permeance and viscosity versus total Hansen solubility parameter for (c) TFP-MPF membrane and (d) the TFP-MP$_{OH}$F membrane.

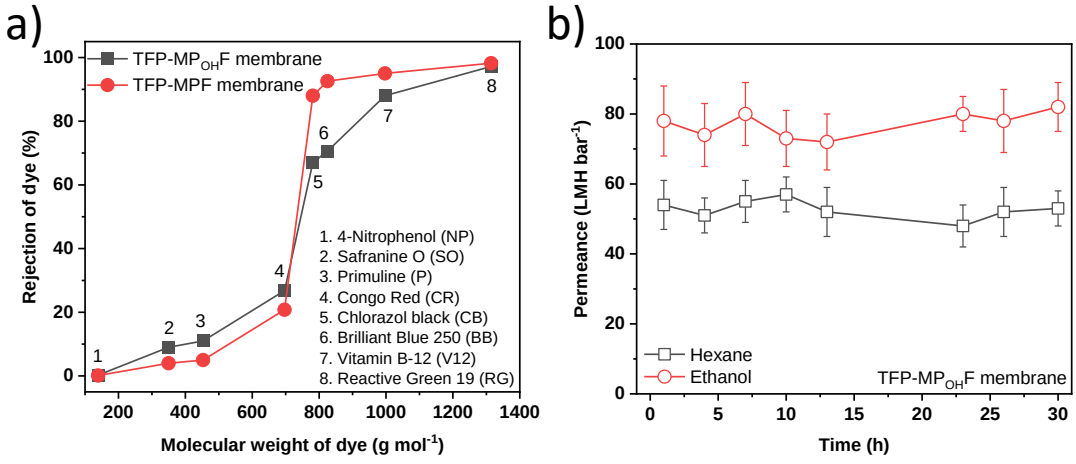

Fig. 6. (a) Dye rejection of TFP-MP$_{OH}$F and TFP-MPF membranes; (b) long-term stability of TFP-MP$_{OH}$F membrane.

The stability of both COF membranes was also assessed. The long-term solvent permeance performance (ethanol and hexane) of the TFP-MP$_{OH}$F membranes was measured to evaluate the membrane stability (Fig. 6b). The results indicated that the permeance was stable for 30 hours of both solvents. The water flux was constant at different pH values, indicating that both COF membranes were stable under acidic and basic conditions (Fig. S8). In addition, thermogravimetric analysis (TGA) confirmed the good thermal stability of both membranes. The membranes were found to be stable up to 350 °C (Fig. S9). These results reveal that the TFP-MP$_{OH}$F and TFP-MPF membranes are thermally and chemically stable and have great potential for solvent nanofiltration and molecular sieving.

4. Conclusions

In summary, we have fabricated two COF membranes with similar pore sizes but distinct chemical structures for OSN applications. The hydroxyl groups in the channel walls make the TFP-MP$_{OH}$F membranes more hydrophilic than TFP-MPF membranes with alkyl chains. As a result, the TFP-MP$_{OH}$F membranes have a higher affinity for polar solvents and exhibit higher permeance, while the relatively hydrophobic inner channels of TFP-MPF membranes facilitate the rapid transport of nonpolar solvents. The organic solvent transport behavior through TFP-MPF membranes follows the pore-flow model, while a deviation was observed for TFP-MP$_{OH}$F membranes,

which is related to the specific interactions between channel walls and solvent molecules. Moreover, both COF membranes showed excellent dye separation performance with a sharp molecular weight cut-off of 800 g mol^{-1} and excellent chemical stability.

Acknowledgments

This work was supported by KAUST Centre Competitive Fund FCC/1/1972-19 and KAUST baseline fund BAS/1/1375-01.

References

[1] D. S. Sholl and R. P. Lively, Seven chemical separations to change the world, Nature 532 (2016) 435-437. DOI: https://doi.org/10.1038/532435a

[2] P. Marchetti, M. F. Jimenez Solomon, G. Szekely and A. G. Livingston, Molecular Separation with Organic Solvent Nanofiltration: A Critical Review, Chem. Rev. 114 (2014) 10735-10806. DOI: https://doi.org/10.1021/cr500006j

[3] I. Sereewatthanawut, F. W. Lim, Y. S. Bhole, D. Ormerod, A. Horvath, A. T. Boam and A. G. Livingston, Demonstration of Molecular Purification in Polar Aprotic Solvents by Organic Solvent Nanofiltration, Org. Process Res. Dev. 14 (2010) 600-611. DOI: https://doi.org/10.1021/op100028p

[4] B. Liang, X. He, J. Hou, L. Li and Z. Tang, Membrane Separation in Organic Liquid: Technologies, Achievements, and Opportunities, Adv. Mater. 31 (2019) 1806090. DOI: https://doi.org/10.1002/adma.201806090

[5] Z. Zhou, X. Li, D. Guo, D. B. Shinde, D. Lu, L. Chen, X. Liu, L. Cao, A. M. Aboalsaud, Y. Hu and Z. Lai, Electropolymerization of robust conjugated microporous polymer membranes for rapid solvent transport and narrow molecular sieving, Nat. Commun. 11 (2020) 5323. DOI: https://doi.org/10.1038/s41467-020-19182-1

[6] S. Karan, Z. Jiang and A. G. Livingston, Sub–10 nm polyamide nanofilms with ultrafast solvent transport for molecular separation, Science 348 (2015) 1347-1351. DOI: 10.1126/science.aaa5058

[7] T. Huang, B. A. Moosa, P. Hoang, J. Liu, S. Chisca, G. Zhang, M. AlYami, N. M. Khashab and S. P. Nunes, Molecularly-porous ultrathin membranes for highly selective organic solvent nanofiltration, Nat. Commun. 11 (2020) 5882. DOI: https://doi.org/10.1038/s41467-020-19404-6

[8] B. Liang, H. Wang, X. Shi, B. Shen, X. He, Z. A. Ghazi, N. A. Khan, H. Sin, A. M. Khattak, L. Li and Z. Tang, Microporous membranes comprising conjugated polymers with rigid backbones enable ultrafast organic-solvent nanofiltration, Nat. Chem. 10 (2018) 961-967. DOI: https://doi.org/10.1038/s41557-018-0093-9

[9] G. M. Shi, Y. Feng, B. Li, H. M. Tham, J.-Y. Lai and T.-S. Chung, Recent progress of organic solvent nanofiltration membranes, Prog. Polym. Sci. 123 (2021) 101470. DOI: https://doi.org/10.1016/j.progpolymsci.2021.101470

[10] H. Wang, M. Wang, X. Liang, J. Yuan, H. Yang, S. Wang, Y. Ren, H. Wu, F. Pan and Z. Jiang, Organic molecular sieve membranes for chemical separations, Chem. Soc. Rev. 50 (2021) 5468-5516. DOI: https://doi.org/10.1039/D0CS01347A

[11] C. Mao, S. Zhao, P. He, Z. Wang and J. Wang, Covalent organic framework membranes with limited channels filling through in-situ grown polyaniline for efficient dye nanofiltration, Chem. Eng. J. 414 (2021) 128929. DOI: https://doi.org/10.1016/j.cej.2021.128929

[12] R. Wang, J. Guo, J. Xue and H. Wang, Covalent Organic Framework Membranes for Efficient Chemicals Separation, Small Struct. 2 (2021) 2100061. DOI: https://doi.org/10.1002/sstr.202100061

[13] J. Kujawa, S. Al-Gharabli, T. M. Muzioł, K. Knozowska, G. Li, L. F. Dumée and W. Kujawski, Crystalline porous frameworks as nano-enhancers for membrane liquid separation – Recent developments, Coord. Chem. Rev. 440 (2021) 213969. DOI: https://doi.org/10.1016/j.ccr.2021.213969

[14] C. Zhang, B.-H. Wu, M.-Q. Ma, Z. Wang and Z.-K. Xu, Ultrathin metal/covalent–organic framework membranes towards ultimate separation, Chem. Soc. Rev. 48 (2019) 3811-3841. DOI: https://doi.org/10.1039/C9CS00322C

[15] D. B. Shinde, G. Sheng, X. Li, M. Ostwal, A.-H. Emwas, K.-W. Huang and Z. Lai, Crystalline 2D Covalent Organic Framework Membranes for High-Flux Organic Solvent Nanofiltration, J. Am. Chem. Soc. 140 (2018) 14342-14349. DOI: https://doi.org/10.1021/jacs.8b08788

[16] S. Zhao, C. Jiang, J. Fan, S. Hong, P. Mei, R. Yao, Y. Liu, S. Zhang, H. Li, H. Zhang, C. Sun, Z. Guo, P. Shao, Y. Zhu, J. Zhang, L. Guo, Y. Ma, J. Zhang, X. Feng, F. Wang, H. Wu and B. Wang, Hydrophilicity gradient in covalent organic frameworks for membrane distillation, Nat. Mater. 20 (2021) 1551-1558. DOI: https://doi.org/10.1038/s41563-021-01052-w

[17] Z. Wang, S. Zhang, Y. Chen, Z. Zhang and S. Ma, Covalent organic frameworks for separation applications, Chem. Soc. Rev. 49 (2020) 708-735. DOI: https://doi.org/10.1039/C9CS00827F

[18] S. Yuan, X. Li, J. Zhu, G. Zhang, P. Van Puyvelde and B. Van der Bruggen, Covalent organic frameworks for membrane separation, Chem. Soc. Rev. 48 (2019) 2665-2681. DOI: https://doi.org/10.1039/C8CS00919H

[19] X. Shi, Z. Zhang, S. Fang, J. Wang, Y. Zhang and Y. Wang, Flexible and Robust Three-Dimensional Covalent Organic Framework Membranes for Precise Separations under Extreme Conditions, Nano Lett. 21 (2021) 8355-8362. DOI: https://doi.org/10.1021/acs.nanolett.1c02919

[20] S. Zhang, S. Zhao, X. Jing, Z. Niu and X. Feng, Covalent organic framework-based membranes for liquid separation, Org. Chem. Front. 8 (2021) 3943-3967. DOI: https://doi.org/10.1039/D0QO01354D

[21] N. A. Khan, R. Zhang, H. Wu, J. Shen, J. Yuan, C. Fan, L. Cao, M. A. Olson and Z. Jiang, Solid–Vapor Interface Engineered Covalent Organic Framework Membranes for Molecular Separation, J. Am. Chem. Soc. 142 (2020) 13450-13458. DOI: https://doi.org/10.1021/jacs.0c04589

[22] J. Liu, G. Han, D. Zhao, K. Lu, J. Gao and T.-S. Chung, Self-standing and flexible covalent organic framework (COF) membranes for molecular separation, Sci. Adv. 6 (2020) eabb1110. DOI: https://doi.org/10.1126/sciadv.abb1110

[23] Y. He, X. Lin, Y. Zhou, J. H. Chen, Z. Guo and H. Zhan, Synthesizing Highly Crystalline Self-Standing Covalent Organic Framework Films through a Homogeneous–Floating–Concentrating Strategy for Molecular Separation, Chem. Mater. 33 (2021) 9413-9424. DOI: https://doi.org/10.1021/acs.chemmater.1c03414

[24] S. Gao, Z. Li, Y. Yang, Z. Wang, Y. Wang, S. Luo, K. Yao, J. Qiu, H. Wang, L. Cao, Z. Lai and J. Wang, The Ionic Liquid–H2O Interface: A New Platform for the Synthesis of Highly Crystalline and Molecular Sieving Covalent Organic Framework Membranes, ACS Appl. Mat. Interfaces 13 (2021) 36507-36516. DOI: https://doi.org/10.1021/acsami.1c08789

[25] A. R. Corcos, G. A. Levato, Z. Jiang, A. M. Evans, A. G. Livingston, B. J. Mariñas and W. R. Dichtel, Reducing the Pore Size of Covalent Organic Frameworks in Thin-Film Composite Membranes Enhances Solute Rejection, ACS Mater. Lett. 1 (2019) 440-446. DOI: https://doi.org/10.1021/acsmaterialslett.9b00272

[26] Y. Zhang, J. Guo, G. Han, Y. Bai, Q. Ge, J. Ma, C. H. Lau and L. Shao, Molecularly soldered covalent organic frameworks for ultrafast precision sieving, Sci. Adv. 7 (2021) eabe8706. DOI: https://doi.org/10.1126/sciadv.abe8706

[27] L.-Y. Chen, Y.-N. Gai, X.-T. Gai, J. Qin, Z.-G. Wang, L.-S. Cui, H. Guo, M.-Y. Jiang, Q. Zou, T. Zhou and J.-G. Gai, Interfacial synthesized covalent organic framework nanofiltration membranes for precisely ultrafast sieving, Chem. Eng. J. 430 (2022) 133024. DOI: https://doi.org/10.1016/j.cej.2021.133024

[28] C. Yin, S. Fang, X. Shi, Z. Zhang and Y. Wang, Pressure-modulated synthesis of self-repairing covalent organic frameworks (COFs) for high-flux nanofiltration, J. Membr. Sci. 618 (2021) 118727. DOI: https://doi.org/10.1016/j.memsci.2020.118727

[29] S. Kandambeth, B. P. Biswal, H. D. Chaudhari, K. C. Rout, S. Kunjattu H., S. Mitra, S. Karak, A. Das, R. Mukherjee, U. K. Kharul and R. Banerjee, Selective Molecular Sieving in Self-Standing Porous Covalent-Organic-Framework Membranes, Adv. Mater. 29 (2017) 1603945. DOI: https://doi.org/10.1002/adma.201603945

[30] K. Dey, M. Pal, K. C. Rout, S. Kunjattu H, A. Das, R. Mukherjee, U. K. Kharul and R. Banerjee, Selective Molecular Separation by Interfacially Crystallized Covalent Organic Framework Thin Films, J. Am. Chem. Soc. 139 (2017) 13083-13091. DOI: https://doi.org/10.1021/jacs.7b06640

[31] D. B. Shinde, L. Cao, X. Liu, D. A. D. Wonanke, Z. Zhou, M. N. Hedhili, M. Addicoat, K.-W. Huang and Z. Lai, Tailored pore size and microporosity of covalent organic framework (COF) membranes for improved molecular separation, J. Membr. Sci. Lett. 1 (2021) 100008. DOI: https://doi.org/10.1016/j.memlet.2021.100008

[32] D. B. Shinde, L. Cao, A. D. D. Wonanke, X. Li, S. Kumar, X. Liu, M. N. Hedhili, A.-H. Emwas, M. Addicoat, K.-W. Huang and Z. Lai, Pore engineering of ultrathin covalent organic framework membranes for organic solvent nanofiltration and molecular sieving, Chem. Sci. 11 (2020) 5434-5440. DOI: https://doi.org/10.1039/D0SC01679A

[33] S. R. Hosseinabadi, K. Wyns, V. Meynen, A. Buekenhoudt and B. Van der Bruggen, Solvent-membrane-solute interactions in organic solvent nanofiltration (OSN) for Grignard functionalised ceramic membranes: Explanation via Spiegler-Kedem theory, J. Membr. Sci. 513 (2016) 177-185. DOI: https://doi.org/10.1016/j.memsci.2016.04.044

[34] A. Buekenhoudt, F. Bisignano, G. De Luca, P. Vandezande, M. Wouters and K. Verhulst, Unravelling the solvent flux behaviour of ceramic nanofiltration and ultrafiltration membranes, J. Membr. Sci. 439 (2013) 36-47. DOI: https://doi.org/10.1016/j.memsci.2013.03.032

[35] W. Wei, J. Liu and J. Jiang, Computational Design of 2D Covalent-Organic Framework Membranes for Organic Solvent Nanofiltration, ACS Sust. Chem. Eng. 7 (2019) 1734-1744. DOI: https://doi.org/10.1021/acssuschemeng.8b05599

[36] P. H. H. Duong, Y. K. Shin, V. A. Kuehl, M. M. Afroz, J. O. Hoberg, B. Parkinson, A. C. T. van Duin and K. D. Li-Oakey, Molecular Interactions and Layer Stacking Dictate Covalent Organic Framework Effective Pore Size, ACS Appl. Mater. Interfaces 13 (2021) 42164-42175. DOI: https://doi.org/10.1021/acsami.1c10866

[37] S. Chandra, T. Kundu, K. Dey, M. Addicoat, T. Heine and R. Banerjee, Interplaying Intrinsic and Extrinsic Proton Conductivities in Covalent Organic Frameworks, Chem. Mater. 28 (2016) 1489-1494. DOI: https://doi.org/10.1021/acs.chemmater.5b04947

[38] S. Kandambeth, A. Mallick, B. Lukose, M. V. Mane, T. Heine and R. Banerjee, Construction of Crystalline 2D Covalent Organic Frameworks with Remarkable Chemical (Acid/Base) Stability via a Combined Reversible and Irreversible Route, J. Am. Chem. Soc. 134 (2012) 19524-19527. DOI: https://doi.org/10.1021/ja308278w